Kranthi Kiran
Sanjay Govindjee
Mohammad R.K. Mofrad

Soft Glassy Rheology and Cytoskeletal Mechanics

IMES
INSTITUTE OF
MECHANICAL SYSTEMS

ETH
Eidgenössische Technische Hochschule Zürich
Swiss Federal Institute of Technology Zurich

Soft Glassy Rheology and Cytoskeletal Mechanics

Kranthi Kiran[1,2], Sanjay Govindjee[2,3,*], Mohammad R.K. Mofrad[1]

[1]Department of Bioengineering, University of California, Berkeley, CA 94720, USA

[2]Department of Civil and Environmental Engineering University of California, Berkeley, CA 94720, USA

[3]Center of Mechanics and Materials Research Center, ETH Zurich, CH-8092, Switzerland

Abstract

Cytoskeleton is a complex structure within the cellular corpus that is responsible for the main structural properties and motilities of cells. There are a wide range of models that have been utilized to understand cytoskeletal mechanics. From this large collection of proposed models, the soft glassy rheological model (originally developed for inert soft glassy materials) has gained a certain traction in the literature due to the close resemblance of its predictions to certain mechanical data collected on cell cultures. Here, we critically review the theory of soft glassy rheology and examine the properties of soft glassy materials and their relation to cytoskeleton. In particular, we examine and comment on the ability of the soft glassy rheological model to replicate experimental data. Further, we comment critically upon fundamental inconsistencies regarding equilibrium and non-equilibrium behavior seen in experiments and theory. We close with some comments of caution and recommendations on future avenues of exploration.

1 Introduction

Cytoskeleton is an integrated system of biomolecules, providing the cell with shape, integrity, and internal spatial organization. It is a three-dimensional network consisting of a complex mixture of actin filaments, intermediate filaments and microtubules that are collectively responsible for the main structural properties and motilities of the cell. A wide range of theoretical models have been proposed for cytoskeletal mechanics, ranging from continuum models for cell deformation to actin filament-based models for cell motility [14, 18]. Numerous experimental techniques have also been developed to quantify cytoskeletal mechanics, typically involving a mechanical perturbation to the cell in the form of either an imposed deformation or force

---

*Corresponding author: gsanjay@ethz.ch

and observation of the static and dynamic response of the cell [6, 14, 18]. These experimental measurements along with new theoretical approaches have given rise to several theories for describing the mechanics of living cells. These theories model the cytoskeleton as elastic, viscoelastic, or poro-viscoelastic continua, tensegrity (tension integrity) networks incorporating discrete structural elements that bear compression, porous gels or most recently as soft glassy materials (SGMs) using the soft glassy rheology (SGR) model [14, 18].

Cytoskeletal mechanics plays a key role in many cellular processes and functions, e.g. in cellular mechanotransduction and motility that involves contraction, spreading, and crawling. Mechanics also plays an important role in cell division and programmed cell death. In this context, rheological properties of cytoskeleton are of utmost importance. Several recent studies have reported on the rheological properties of cytoskeleton, in particular examining the frequency dependency of the storage modulus, $G^{'}(\omega)$, and the loss modulus, $G^{''}(\omega)$. Of particular interest are recent experiments that probe the response of the cytoskeleton in the frequency range of 10^{-2} to 10^{3} Hz [6, 3, 5]. Inspired by the similarity between experimental data on cells and those reported on soft glassy materials, Fabry *et al.* [6] hypothesized that the cytoskeleton is a SGM and can be modeled using the SGR model [23].

SGMs form a class of materials that generically include (liquid) foams, emulsions, slurries and pastes. The dynamics and rheological properties of this class of materials have been reasonably well studied; see e.g. [15, 12, 13, 16, 20, 11, 17]. The linear viscoelastic properties of these materials such as the storage modulus and the loss modulus and their dependency on frequency are often measured. Two common features of SGMs, which are observed to some degree in certain frequency ranges, are:

1. The loss tangent $\tan(\bar{\delta}) = G^{''}(\omega)/G^{'}(\omega)$ is nearly constant for a wide range of frequencies, and

2. The frequency dependencies of these moduli are weak power laws of the frequency of the applied load.

The abstract system properties that are claimed to characterize the dynamics of soft glassy systems are the degree of structural disorder and metastability [24]. Many experiments have been performed to show evidence of these generic properties along with notions of aging and rejuvenation; see e.g. [4, 27, 22].

One key characteristic of glassy materials is that they are not in thermodynamic equilibrium below their glass transition temperature. Such materials are regarded as solidified supercooled liquids whose volume, and enthalpy are greater than they would be in the equilibrium state (see Fig.1). The non-equilibrium state is only metastable. Volume-relaxation studies of
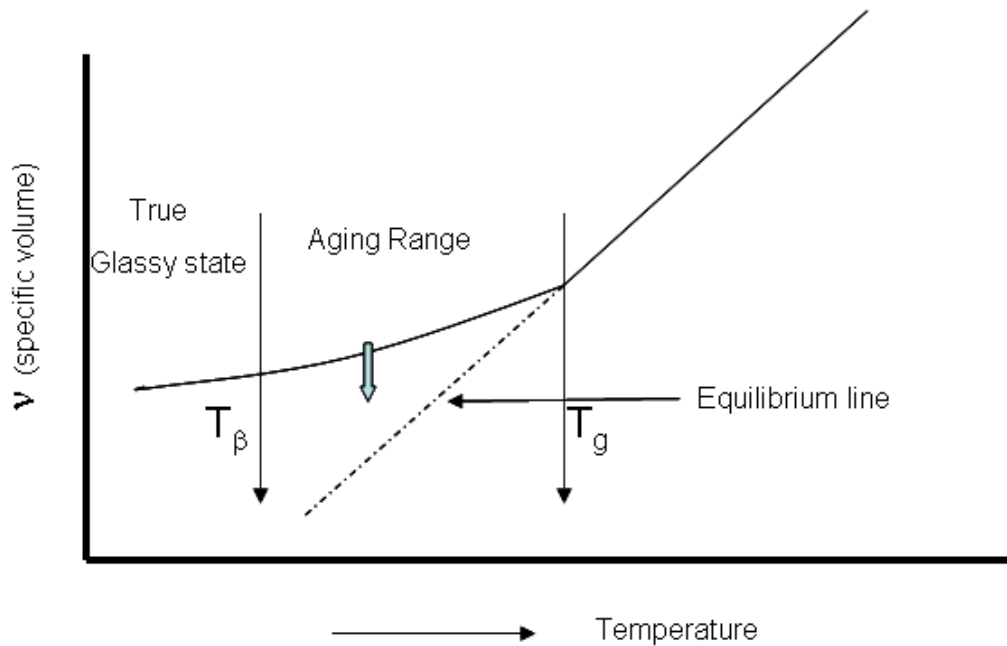
3

Figure 1: Aging schematic. T_g is the glass transition temperature, T_β is the temperature of highest secondary transition and ν is the specific volume.

glassy materials show they undergo slow processes indicating that even below T_g molecular mobility is not fully suppressed. This gradual evolution affects many properties of the material [25]. These properties change with time and the material is said to undergo aging or more precisely 'physical aging'. The main idea of aging in soft glassy materials is that the material properties change with the waiting time after formation of the material. Some of the experiments on SGMs in the literature indicate behavior of this type [4, 22]. Based on such observations of dynamic moduli and aging, Sollich [24, 23] has developed a theory to model soft glassy materials through a modification of Bouchaud's model of traps and glass phenomenology [2, 19].

The objective of this paper is to explore Sollich's theory of soft glassy materials and its relation to cytoskeletal mechanics. We will conclude by raising some open questions that can be useful in the understanding of cytoskeletal dynamics. To begin, in Section 2, we review some rheological representation results which are useful for discussing and understanding the behavior of the cytoskeleton. In Section 3, we review the results of some selected experiments on cytoskeleton. Section 4 examines the model developed by Bouchaud followed by the theory of soft glassy materials proposed by Sollich. The comparison of experimental results to the theory of soft glassy materials is made and analyzed in Section 5.

4

2 Rheological Measures: A Synopsis

A basic knowledge of rheology is essential for an understanding of the meaning of mechanical experiments performed on cell cultures. In this section we provide a summary of a number of important rheological representation results with added remarks on important modeling assumptions. The aim is to provide a context for a reasoned discussion of the SGR model and a common linguistic platform for discussing and interpreting recent measurements on cell cultures. In the interest of brevity we omit the derivations of the presented formulae and simply refer the interested reader to the classic references [8, 26]. Not all which we present can be found in these references, but from them, and some modest complex-variable theory, one can derive all the presented results.

2.1 Generic response functional representations

In the interest of illuminating rheological issues, we make our presentation strictly within the geometrically linear theory. In this context, the appropriate strain measure is

$$\boldsymbol{\varepsilon} = \frac{1}{2}(\nabla \boldsymbol{u} + \nabla \boldsymbol{u}^T), \tag{1}$$

the symmetric displacement gradient. Within this realm, the simplest material response is stress $\boldsymbol{\sigma} = \hat{\boldsymbol{\sigma}}(\boldsymbol{\varepsilon})$, such that $\int_{t_1}^{t_2} \boldsymbol{\sigma} : \dot{\boldsymbol{\varepsilon}}\, dt = 0$, where $\boldsymbol{\varepsilon}(t_1) = \boldsymbol{\varepsilon}(t_2)$. The salient feature of this model is that the stress is an instantaneous function of the present value of the strain and is unaffected by the past history. In short, the material is elastic.

In a viscoelastic setting, the stress is dependent on the current and also on the past history of the strain; i.e.,

$$\boldsymbol{\sigma}(t) = \underset{t' \in (-\infty, t]}{\mathfrak{S}} (\boldsymbol{\varepsilon}(t')). \tag{2}$$

The stress is said to be a functional of the strain history. Within reasonable continuity assumptions, one can expand the functional as a functional polynomial [10]. Retaining the leading two terms and assuming the material possesses time translational invariance (TTI) gives us the classic expression

$$\boldsymbol{\sigma}(t) = \int_{-\infty}^{t} \mathbb{C}(t - t') : \frac{d\boldsymbol{\varepsilon}}{dt'}\, dt'. \tag{3}$$

Here, $\mathbb{C}(t)$ is the fourth order tensorial relaxation kernel. We can additionally split the response into volumetric and deviatoric parts using the standard definitions: $\boldsymbol{\sigma} = p\mathbf{1} + \boldsymbol{s}$, where the deviatoric stress $\boldsymbol{s} = \boldsymbol{\sigma} - \frac{1}{3}\mathrm{tr}(\boldsymbol{\sigma})\mathbf{1}$

and the pressure $p = \frac{1}{3}\text{tr}(\boldsymbol{\sigma})$. If we make the further assumption of isotropy and elastic bulk response, then, constitutively, we have

$$p = \kappa \, \text{tr}(\boldsymbol{\varepsilon})$$

$$\boldsymbol{s}(t) = \int_{-\infty}^{t} G(t - t')\frac{d\boldsymbol{e}}{dt'} \, dt' \,, \tag{4}$$

where κ is the bulk modulus and $\boldsymbol{e} = \boldsymbol{\varepsilon} - \frac{1}{3}\text{tr}(\boldsymbol{\varepsilon})\mathbf{1}$ is the deviatoric strain. Thus, in the linear isotropic setting with elastic bulk response, complete specification of the mechanical rheological properties reduces to the determination of $G(\cdot)$, the so-called (shear) relaxation modulus.

Remarks:

1. It should be emphasized that the representation in Eq. (3) presumes the notion of TTI. This is a very central assumption in most rheological models. Thus care must be taken when trying to interpret results that may pertain to out of equilibrium systems where TTI is no longer generally valid. When TTI does not hold, we have the added complication that the relaxation modulus depends not only on $t - t'$ but also explicitly upon t' – i.e. $G(t - t', t')$.

2. Eqs. (3) and (4) represent models that have a rather broad range of applicability. They are fully independent of any physical model of relaxation and evolution of microstructure. In particular they are appropriate for stress determination for essentially arbitrary strain histories. This is a point that should be kept in mind when thinking about using rheological models within larger modeling frameworks such as physiological response simulation systems of whole organs or larger systems [21]. For these purposes, $G(t)$ is generally required and must be defined over the range $t \in [0, \infty)$.

3. The value $G(0)$ is the instantaneous elastic modulus and can be relatively quite high. In fact $G(0) = \infty$ can be mathematically sound but is of course physically unrealistic. For models permitting $G(0) = \infty$, care must be taken in limiting the strength of the singularity so that the required integrals are well defined.

4. $G(t)$ needs to possess the so-called fading memory property. To first order, this requires that $G(t) \to G_\infty$, a constant as $t \to \infty$. If $G_\infty = 0$, then material is considered a viscoelastic fluid, otherwise a viscoelastic solid.

5. The use of viscoelastic internal variables with differential evolution laws is an alternative to the modeling framework of Eqs. (3) and (4). However, it should be noted that such models are, in principal for the geometrically linear case, a subset of the convolution type models.

2.2 Experimental Methods

In theory, the easiest way to determine $G(t)$ is to perform a shear test by imposing a deviatoric step strain $\boldsymbol{e}(t) = \boldsymbol{e}_0 H(t)$, where $\mathrm{tr}(\boldsymbol{e}_0) = 0$ and $H(t)$ is the Heaviside step function. In this case, the measured stress response, $\boldsymbol{s}(t) = G(t)\boldsymbol{e}_0$, directly provides the relaxation function. In practice the imposition of a step strain involves a time constant for inducing the motion and a sampling rate. The net result is that $G(t)$ will only be known in some time interval $[t_{\min}, t_{\max}]$. However, for a complete theory, one must extend the domain to $[0, \infty)$. For a variety of reasons, not the least of which is experimental fidelity, one often employs steady state excitation to determine $G(t)$. In this case, one ends up measuring a near relative of the Fourier transform of $G(t)$. Let $\boldsymbol{e}(t) = \boldsymbol{e}_0 \exp[i\omega t]$, where $i = \sqrt{-1}$ and ω is the frequency of the imposed deformation. Then from Eq. (4), $\boldsymbol{s}(t) = G^*(\omega)\boldsymbol{e}(t)$, where $G^*(\omega)$ is known as the dynamic or complex modulus. $G^{'}(\omega) = \mathrm{Re}(G^*(\omega))$ provides the in-phase stiffness or storage modulus and $G^{''}(\omega) = \mathrm{Im}(G^*(\omega))$ is the out-of-phase stiffness or loss modulus. Their ratio $G^{''}/G^{'}$ is referred to as the loss tangent, $\tan(\bar{\delta}(\omega))$, and is the easiest of all the linear rheological functions to measure as $\bar{\delta}(\omega)$ is just the phase lag of the stress response to the strain excitation. In such experiments $|G^*|$ is the ratio of the peak stress to peak strain. Thus one also has $G^{'} = |G^*|\cos(\bar{\delta})$ and $G^{''} = |G^*|\sin(\bar{\delta})$.

2.3 Interconversion Relations

Knowledge of the steady state response (in analytic form) can be used to determine the actual (needed) relaxation function and vice-versa. Useful forms for going from $G(t)$ to the steady state forms are

$$G^*(\omega) = i\omega \int_0^\infty G(t')e^{-i\omega t'}\, dt',$$

$$G^{'}(\omega) = \omega \int_0^\infty G(t')\sin(\omega t')\, dt', \tag{5}$$

$$G^{''}(\omega) = \omega \int_0^\infty G(t')\cos(\omega t')\, dt'.$$

If one defines the Laplace transform of $G(t)$ as $\mathfrak{L}G(p) = \int_0^\infty G(t)e^{-pt}\, dt$, then one also has the compact representation

$$G^*(\omega) = p\mathfrak{L}G(p)\Big|_{p=i\omega}. \tag{6}$$

The reverse forms are easily derivable via inverse transforms of Eqs. (5):

$$G(t) = \frac{1}{2\pi} \int_{-\infty}^{\infty} \frac{G^*(\omega)}{i\omega} e^{i\omega t} \, d\omega,$$

$$G(t) = \frac{2}{\pi} \int_{0}^{\infty} \frac{G'(\omega)}{\omega} \sin(\omega t) \, d\omega, \tag{7}$$

$$G(t) = \frac{2}{\pi} \int_{0}^{\infty} \frac{G''(\omega)}{\omega} \cos(\omega t) \, d\omega.$$

Remarks:

1. Implicit in Eqs. (5), (6) and (7) is the requirement that the needed integrals exist. This puts limits on possible forms for $G(t)$. For example, the popular form $G(t) = t^{-p}$, requires $0 < p < 1$. In this case, $G^*(\omega) = (-1)^{p-1}\Gamma(1-p)(i\omega)^p$, where $\Gamma(\cdot)$ is the Gamma-function.

2.4 Spectral Forms

A common method of understanding and interpreting relaxation kernels is via spectra. From a purely mathematical perspective, independent of any micro-physical models, we can express $G(t)$ as

$$G(t) = \int_{0}^{\infty} F(\tau)e^{-\frac{t}{\tau}} \, d\tau, \tag{8}$$

where $F(\tau)$ is known as the relaxation-time spectrum for $G(t)$. The form is quite general and is not restricted to overall exponential relaxation as one may naively presume from Eq. (8). However, it is common for one to refer to $F(\cdot)$ as a distribution of Maxwell modes. The specification of $F(\cdot)$ allows one to think of relaxation mechanisms in a continuous sense. This is a point which makes good physical sense, if one truly contemplates the number of possible relaxation mechanisms in any finite size sample. Other common alternatives to Eq. (8) express $G(t)$ in terms of log relaxation-time and relaxation-frequency spectra:

$$G(t) = \int_{-\infty}^{\infty} H(\log \tau)e^{-\frac{t}{\tau}} \, d(\log \tau), \tag{9}$$

where $H(\log \tau)/\tau = F(\tau)$ and

$$G(t) = \int_{0}^{\infty} N(\alpha)e^{-t\alpha} \, d\alpha, \tag{10}$$

where $N(1/\tau)/\tau^2 = F(\tau)$. The spectra can also be used to define the steady-state response functions. In particular we also have:

$$
\begin{aligned}
G^*(\omega) &= \int_0^\infty F(\tau)\frac{(\omega\tau)^2 + i\omega\tau}{1 + (\omega\tau)^2}\,\mathrm{d}\tau, \\
&= \int_{-\infty}^\infty H(\log\tau)\frac{(\omega\tau)^2 + i\omega\tau}{1 + (\omega\tau)^2}\,\mathrm{d}(\log\tau), \\
&= \int_0^\infty N(\alpha)\frac{\omega^2 + i\omega\alpha}{\alpha^2 + \omega^2}\,\mathrm{d}\alpha,
\end{aligned}
\tag{11}
$$

with

$$
\begin{aligned}
G'(\omega) &= \int_0^\infty F(\tau)\frac{(\omega\tau)^2}{1 + (\omega\tau)^2}\,\mathrm{d}\tau, \\
&= \int_{-\infty}^\infty H(\log\tau)\frac{(\omega\tau)^2}{1 + (\omega\tau)^2}\,\mathrm{d}(\log\tau), \\
&= \int_0^\infty N(\alpha)\frac{\omega^2}{\alpha^2 + \omega^2}\,\mathrm{d}\alpha,
\end{aligned}
\tag{12}
$$

and

$$
\begin{aligned}
G''(\omega) &= \int_0^\infty F(\tau)\frac{\omega\tau}{1 + (\omega\tau)^2}\,\mathrm{d}\tau, \\
&= \int_{-\infty}^\infty H(\log\tau)\frac{\omega\tau}{1 + (\omega\tau)^2}\,\mathrm{d}(\log\tau), \\
&= \int_0^\infty N(\alpha)\frac{\omega\alpha}{\alpha^2 + \omega^2}\,\mathrm{d}\alpha.
\end{aligned}
\tag{13}
$$

The log relaxation-time spectra in terms of the steady-state response functions can be determined using the technique of [9] as:

$$
\begin{aligned}
H(\log\tau) &= \frac{i}{\pi}\left[G'\left(\frac{1}{\tau}e^{i\frac{\pi}{2}}\right) - G'\left(\frac{1}{\tau}e^{-i\frac{\pi}{2}}\right)\right], \\
&= \frac{1}{\pi}\left[G''\left(\frac{1}{\tau}e^{i\frac{\pi}{2}}\right) + G''\left(\frac{1}{\tau}e^{-i\frac{\pi}{2}}\right)\right].
\end{aligned}
\tag{14}
$$

Expressions in terms of the complex modulus can be obtained by simply noting that the storage and loss moduli are, respectively, the real and imaginary parts of the complex modulus. Further, with knowledge that $N(1/\tau) = \tau H(\log\tau)$ and $F(\tau) = H(\log\tau)/\tau$ the other two spectra can be determined. To find the spectra in terms of the temporal relaxation function, one needs to additionally apply Eq. (5).

3 Experiments on Cytoskeleton

3.1 Equilibrium Rheological Measurements

Fabry *et al.* [6] have performed experiments on the mechanical response of cellular cytoskeleton with an eye towards soft glassy rheology and thus we will focus our discussions mainly upon their data. They have obtained the mechanical response of a variety of cells through magnetic twisting cytometry (MTC); see Fig. 2. The details of the experiments are given in [6]. The dynamic properties G' and G'' of the cytoskeleton's structural response were measured in the experiments; see Fig. 3. It should be remarked that the measured mechanical properties correspond to the linear mechanical behavior of the cytoskeleton embedded inside a cell and are, as such, not the "true" moduli of the cytoskeleton in the sense of a homogenized continuum – though, by linearity, one can reasonably argue that the properties reported should be linearly proportional to the true homogenized continuum moduli of the cytoskeleton.

In the experiments mentioned, the magnetic bead is attached to the cytoskeleton via rigid links between transmembrane integrins and the extracellular molecules (e.g. fibronectins) that are coated on the bead (Fig. 2). A magnetic twisting field introduces a torque causing the bead to rotate and to displace (Fig. 2). The frequency dependence of G' and G'' is then extracted from the structural response at the point of bead attachment. The results are as shown in Fig. 3, where G' increases with increasing frequency, ω, according to a power law $\sim \omega^{x-1}$, with $x = 1.20$ under control conditions. G'' also increases with increasing frequency and follows the same power law in the range of 0.01 to 10 Hz. Above 10 Hz, however, the same power law behavior is *not* seen. Similar experiments were performed by manipulating the cells with various drugs in order to create contraction or relaxation in the cytoskeleton and identical qualitative properties were again observed (Fig. 3). G' increased with increasing frequency, ω, as a power law $\sim \omega^{x-1}$ but with different values of x for each treatment. The value of x correlated sensibly to the biochemical activity of the drug. G'' also increased with increasing frequency with the same power law and same exponent until 10 Hz; above 10 Hz, the behavior changed in a manner similar to what was observed in the control. It was also noted that the loss tangent in the frequency range 0.01 to 10 Hz was relatively frequency insensitive and was of the order of 0.1.

Fabry *et al.* [7] proposed an empirical relationship for the data they observed from the experiments. They proposed that the stress response $G(t)$ to a unit step strain imposed on the cell at t=0 is:

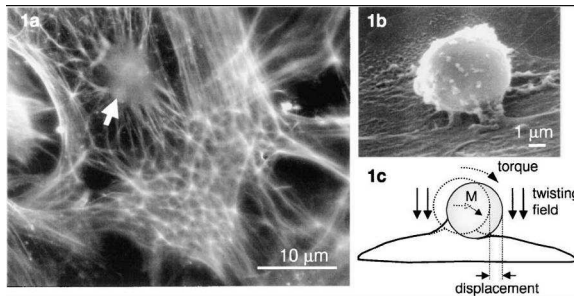$$G(t) = \mu\delta(t) + \hat{G}\left(\frac{t}{\hat{t}}\right)^{1-x}, \quad t \geq 0. \tag{15}$$

Figure 2: (a) and (b) Beads attached to the cytoskeleton. (c) The application of magnetic field and the displacement of the bead [7] (reproduced with permission).

Here, $\hat{G}$ is the ratio of stress to the unit strain measured at an arbitrarily chosen time $\hat{t}$, μ is a Newtonian viscosity, and $\delta(\cdot)$ is the Dirac delta function. The complex-valued dynamic modulus for this model is:

$$G^*(\omega) = i\omega\mu$$
$$+ \hat{G}\left(\frac{i\omega}{\hat{\Phi}}\right)^{x-1} \Gamma(2-x)\left[\cos\left(\frac{\pi}{2}(x-1)\right) + i\sin\left(\frac{\pi}{2}(x-1)\right)\right], \quad (16)$$

where $\hat{\Phi} = \hat{t}^{-1}$. The expression is mathematically valid for $x < 2$ but the physical restriction (of fading memory) that the relaxation function should not grow with time imposes the limit $x > 1$. Thus, the relations should only be considered valid for $1 < x < 2$. It should also be noted that the relaxation function, Eq. (15), presumes TTI. Thus, the dynamic modulus, Eq. (16) should also be considered to assume TTI; i.e. both relations are really only valid near thermodynamic equilibrium.

Equation (16) is a remarkably good fit of the data obtained from the experiments and the values of the 4 parameters μ, $\hat{G}$, $\hat{\Phi}$ and x can be obtained by statistical analysis of the data. It is striking that drug interactions only seem to effect x when dealing with a single class of cells. As we shall see in Section 4, the empirically assumed forms Eqs. (15) and (16) bear a very close resemblance to the SGR model equations.

4   Soft Glassy Materials

4.1   Bouchaud's Glass Model

Bouchaud originally studied the concepts of structural disorder and metastable configurations in spin-glasses [2], and later applied his ideas to explain the phenomenology of glassy systems in general [19]. This model of glass phenomenology is discussed here as it leads directly to Sollich's rheological theory of soft glassy materials. The conformational energy landscape of a finite
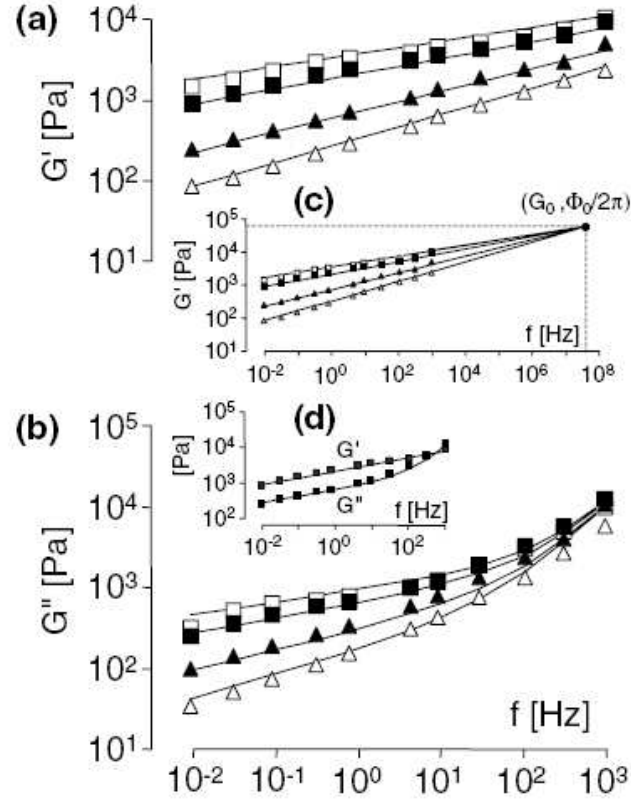
11

Figure 3: (a) and (b) G' and G'' as a function of frequency ω for different drug treatments. Under controlled conditions (filled squares), treatment with histamin (unfilled squares), treatment with DBcAMP (filled triangles), treatment with Cytochalasin D (unfilled triangles). The solid lines are fit using Eq. (16) with the values of $\hat{G} = 53.6$ kPa, $\hat{\Phi} = 25 \times 10^7$ rad/s and $\mu = 1.41$ Pa $\cdot$ s. (c) Extrapolation of solid lines cross over at $(\hat{G}, \hat{\Phi})$. (d) Dynamic moduli under control conditions [7] (reproduced with permission).
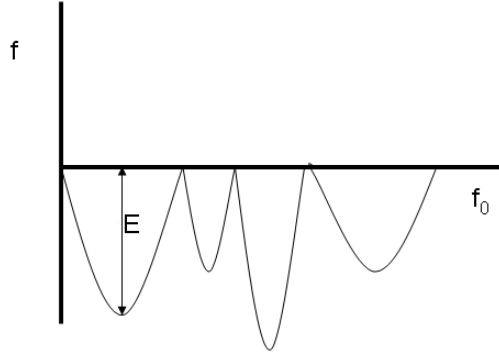
Figure 4: Energy landscape showing different metastable states (after [2]).

disordered system is extremely rough, with many local minima corresponding to metastable configurations, or states. These local minima are assumed to be surrounded by high energy barriers. These states can thus be considered as traps which hold the system for certain periods of time τ. The distribution of these trapping times is critical in the quantification of such materials.

A schematic of the energy landscape is given in Fig. 4. Here, f_0 is the energy level below which the states are disconnected. It is the minimum energy required to hop between any two states. It is assumed here that the dynamics between the traps is very fast and the probability to find the system between two metastable states is negligible. The depth of a trap is $E = f_0 - f > 0$. In the model, the abstract space of traps is characterized by a given probability density function $\rho(E)$ for the depth of the traps. Assuming a canonical distribution at temperature $T = \beta^{-1}$, the system can escape from its trap of depth E with a rate $\Gamma_0 e^{-\beta E}$ per unit time, where Γ_0 is an attempt rate. The system chooses a new trap of depth E' with probability $\rho(E')$, with no reference to any spatial structure as may be implied by Fig. 4. Therefore, the probability $P(E, t)$ that one can find the system in a trap of energy depth E at time t evolves in time from an initial condition $P_0(E)$ according to the master balance equation as

$$\frac{\partial P(E, t)}{\partial t} = -\Gamma_0 e^{-\beta E} P(E, t) + \Gamma_0 \Gamma(t) \rho(E), \qquad (17)$$

where $\Gamma(t) = \int_0^\infty e^{-\beta E} P(E, t) \, dE$ and a Boltzmann temperature scale is presumed. On the right hand side of Eq. (17), the first term indicates the

13

rate of probability of hopping out of a trap of energy depth E. The second term indicates the rate of probability of the system falling into a trap of energy depth E. Taken together, these two terms give the rate of change of the probability of finding the system in a trap of depth E.

A normalizable stationary distribution $P_{eq}(E)$ exists at temperature $T = \beta^{-1}$ if and only if

$$\Gamma_{eq}(\beta) = \frac{1}{\int_0^\infty e^{\beta E} \rho(E)\, dE} > 0. \tag{18}$$

If we have a normalizable stationary distribution, then $P_{eq}(E)$ is given by

$$P_{eq}(E) = \Gamma_{eq}(\beta) e^{\beta E} \rho(E). \tag{19}$$

The condition of normalizability is closely related to the large energy asymptotic behavior of the distribution of traps, which is characterized by the reciprocal (glass transition) temperature:

$$\frac{1}{T_g} = \beta_g = \lim_{E \to \infty} -\frac{\log(\rho(E))}{E}. \tag{20}$$

As pointed out by Bouchaud, three interesting cases arise from this criterion:

1. If $\rho(E)$ decays faster than exponentially at large E, then $T_g = 0$ and a normalizable stationary distribution always exists.

2. If $\rho(E)$ decays slower than exponentially at large E, then $T_g = \infty$ and a normalizable stationary distribution does not exist.

3. If $\rho(E)$ decays exponentially as $e^{-\beta_g E}$ at large E, then T_g is finite and a normalizable stationary distribution exists at temperatures above T_g.

These are the central elements of the Bouchaud's abstract model. Before going on to discuss the theory proposed by Sollich, it is important to state that Sollich assumes the existence of a finite non-zero glass transition temperature such that a normalizable stationary distribution exists above a finite T_g and ceases to exist below it.

4.2 Soft Glassy Rheology Theory

Based on Bouchaud's glass model, Sollich [24, 23] proposed the soft glassy rheology (SGR) model. The model pictures a material which consists of a large number of elements that are trapped in "cages" formed by their neighbors. An individual element sees an energy landscape of traps of various depths and, when activated, hops into another trap. Sollich claims that in soft glassy materials, thermal activation is, a priori, very small compared to the typical trap depths. Sollich further claims that activation is due to the

interactions between elements; i.e., rearrangements somewhere in the material can cause rearrangements elsewhere. This coupling between elements is unspecified in the model and is solely represented by an effective abstract noise temperature x [24, 23]. In reality, it is more likely that the energy barriers are changing due to rearrangements – for example as is known to happen in the yielding of glassy polymers [1]. However, since only the ratio of the energy barrier to the temperature appears in the SGR theory, one can argue that one does not have to specify the true state of affairs.

Sollich's evolution equation for the probability of finding an element in a trap of depth E at time t is similar to Eq. (17), except with β replaced by $1/x$. Thus similar to the three cases considered by Bouchaud, to have a normalizable probability distribution, one also has here three cases with x_g being zero, infinite and finite. As mentioned, Sollich assumes that there exists a finite value for the glass transition, denoted here by x_g. For x above x_g, a stationary probability distribution exists and will be reached after a certain amount of time, and below x_g the stationary probability distribution ceases to exist. Thus Sollich assumes the density of traps has an exponential tail, $\rho(E) \sim \exp[-E/x_g]$.

In order to describe material deformation and flow, Sollich further incorporates strain degrees of freedom into Bouchaud's model as a bias on the trapping depths. He restricts himself to a one-dimensional model and introduces a local scalar strain variable l per element. Applying a strain on the material, each element is assumed to deform elastically from the local equilibrium configuration until it reaches a yield point, identified by l_y, from where the element rearranges into a new configuration relaxing the stress in the element. It is assumed that the element fully relaxes taking the strain completely back to zero. As the macroscopic strain γ is increased, l executes a sawtooth-like motion. The yield strain l_y is obtained from the trap depth E, in which the element is located, and thus the yield points have a distribution and not a single value.

Assuming each element to be linearly elastic with an elastic constant k, the stress in the elements evolves as kl, and the elastic energy that can be stored in an element is $\frac{1}{2}kl_y^2$. Assuming that the microscopic strain rate is the same as the macroscopic strain rate, $\dot{\gamma}$, the state of the system at time t is characterized by the probability of finding an element in a trap of energy depth E and a local strain l at time t. The probability evolves as

$$\frac{\partial P(E,l,t)}{\partial t} = -\dot{\gamma}\frac{\partial P}{\partial l} - \Gamma_0 e^{-\frac{E-\frac{1}{2}kl^2}{x}} P + \Gamma_0 \Gamma(t)\rho(E)\delta(l), \qquad (21)$$

where

$$\Gamma(t) = \int\int e^{-\frac{E-\frac{1}{2}kl^2}{x}} P(E,l,t)\,dl\,dE. \qquad (22)$$

On the right hand side of Eq. (21), the first term represents the change in probability because of the motion in the same energy trap E, while the

second and third terms have the same meaning as described earlier. Note that the third term now contains a $\delta(l)$ function, due to the assumption that the local strain becomes zero immediately after the relaxation. It must be remarked that the energy well chosen is uncorrelated with its previous one. The average non-dimensionalized (by Γ_0) yielding rate is given by Eq. (22).

Finally, the rheological response, which is the macroscopic stress, is obtained as the expectation value of the local stresses:

$$\sigma = \int \int klP(E,l,t)\,dl\,dE. \tag{23}$$

As Sollich importantly points out, the "effective noise" temperature x is not a parameter that we can easily tune from outside; rather, it is to be determined self-consistently by the interactions in the system.

4.3 Constitutive Equation

The relation between stress and strain allows one to make a direct comparison of the soft glassy model to experiments on cytoskeleton. In this section, we follow Sollich's argument to obtain the constitutive equation at the macroscopic level by considering the mesoscale dynamics.

By considering the initial state to be completely unstrained $\gamma(0) = 0$, and the initial probability distribution as

$$P(E,l,t=0) = P_0(E)\delta(l)\,, \tag{24}$$

Equation (21) can be solved and the macroscopic stress can be obtained in terms of the macroscopic strain $\gamma(t)$ and the effective temperature x:

$$\sigma(t) = k\gamma(t)G_0(Z(t,0)) + \Gamma_0 \int_0^t \Gamma(t')[\gamma(t) - \gamma(t')]G_\rho(Z(t,t'))\,dt', \tag{25}$$

$$1 = G_0(Z(t,0)) + \Gamma_0 \int_0^t \Gamma(t')G_\rho(Z(t,t'))\,dt', \tag{26}$$

$$G_0(z) = \int P_0(E)e^{-ze^{-\frac{E}{x}}}\,dE, \tag{27}$$

$$G_\rho(z) = \int \rho(E)e^{-ze^{-\frac{E}{x}}}\,dE\,. \tag{28}$$

Equation (25) represents the evolution of the macroscopic stress with respect to time. The determination of the average yielding rate can be found from (26). The noise induced decay of the stress is represented by Eqs. (27) and (28) and is governed by the effective time interval given by:

$$z = Z(t,t') = \Gamma_0 \int_{t'}^t e^{\frac{[\gamma(t'')-\gamma(t')]^2}{2x}}\,dt''. \tag{29}$$

The first term on the right hand side of Eq. (25) is the contribution of elements that have not yielded from time 0 to t. The second term integrates the contributions from all elements that have yielded at least once between time 0 and t.

4.4   Small Strain SGR

Since our focus is on the small strain rheology of the cytoskeleton, we limit our examination of Sollich's model to the linear regime. If we linearize Eq. (29) with respect to the strain, then we find a dominant $O(1)$ term leading to the simplification that $Z(t, t') = \Gamma_0(t - t')$. This is the case where strain induced yielding is negligible; i.e., all yield events are noise induced. For the moment, let us consider the case above the glass transition; i.e., for $x > x_g$. The equilibrium distribution at that particular value of x and $\gamma(0) = 0$ is chosen for the initial distribution of energies; i.e., we start with the material being in an equilibrium state above its glass transition. From now on, the distribution of energies $\rho(E)$ has the particular form $\rho(E) = (1/x_g) \exp[-E/x_g]$. Thus,

$$P_0(E) = P_{eq}(E) = \Gamma_{eq} e^{\frac{E}{x}} \rho(E) = \Gamma_{eq} \frac{1}{x_g} e^{-\frac{E}{x}\left(\frac{x}{x_g} - 1\right)} \tag{30}$$

With Eq. (30), $G_0(z)$ and $G_\rho(z)$ can be related and the value of Γ_{eq} can be obtained as:

$$G_\rho(z) = -\Gamma_{eq}^{-1} \frac{d}{dz}(G_0(z)), \tag{31}$$

$$\Gamma_{eq}^{-1} = \int \rho(E) e^{\frac{E}{x}} dE = \frac{x}{x - x_g}. \tag{32}$$

The average non-dimensional yielding rate is found to be $\Gamma(t) = \Gamma_{eq}$ from Eqs. (26)–(28).

Finally Eq. (25) can be reduced to:

$$\sigma(t) = k \int_0^t G_0(\Gamma_0(t - t')) \frac{d\gamma}{dt'} dt'. \tag{33}$$

From Eq. (33) we can identify the relaxation modulus of the model as

$$G(t) = kG_0(\Gamma_0 t) = k\Gamma_0 \left(\frac{x}{x_g} - 1\right) \int_{1/\Gamma_0}^{\infty} e^{-t/\tau} (\Gamma_0 \tau)^{-x/x_g} d\tau, \tag{34}$$

where we have employed the change of variables $\tau = (1/\Gamma_0) \exp(E/x)$ which, in the SGR model, represents the average trapping time in a particular well. The dependency of the dynamic modulus on frequency is obtained as

$$G^*(\omega) = G'(\omega) + iG''(\omega) = i\omega \int_0^{\infty} e^{-i\omega t} kG_0(\Gamma_0 t)\, dt$$
$$= k\Gamma_0 \left(\frac{x}{x_g} - 1\right) \int_{\frac{1}{\Gamma_0}}^{\infty} \frac{i\omega\tau}{1 + i\omega\tau} (\Gamma_0 \tau)^{-\frac{x}{x_g}} d\tau. \tag{35}$$

Remarks:

1. In reference to Section 2.4, Eqs. (34) and (35) show that the linearized near equilibrium SGR model is mathematically equivalent to a system (of Maxwell elements) with a continuous power law distribution of relaxations times, $F \sim \tau^{-x/x_g}$, and a lower relaxation time cut-off of $1/\Gamma_0$. In relaxation space, we see that this model has a linear distribution on a $\log - \log$ scale; i.e. $\log(H) \sim \log(\tau)$.

2. The behavior of the dynamic modulus is most easily seen via simple numerical simulation; see Figs. 5 and 6 . One observes for frequencies of order 1 and less relative to the attempt frequency, Γ_0 that:

$$
G'(\omega) \sim \begin{cases} \left(\frac{\omega}{\Gamma_0}\right)^2 & \text{for } 3 < \frac{x}{x_g} \text{ and } 10^{-4} < \frac{\omega}{\Gamma_0} < 1 \\ \left(\frac{\omega}{\Gamma_0}\right)^{(x/x_g)-1} & \text{for } 1 < \frac{x}{x_g} < 3 \text{ and } 10^{-4} < \frac{\omega}{\Gamma_0} < 1, \end{cases} \tag{36}
$$

$$
G''(\omega) \sim \begin{cases} \left(\frac{\omega}{\Gamma_0}\right) & \text{for } 2 < \frac{x}{x_g} \text{ and } 10^{-4} < \frac{\omega}{\Gamma_0} < 1, \\ \left(\frac{\omega}{\Gamma_0}\right)^{(x/x_g)-1} & \text{for } 1 < \frac{x}{x_g} < 2 \text{ and } 10^{-4} < \frac{\omega}{\Gamma_0} < 1. \end{cases} \tag{37}
$$

   When x/x_g approaches 1, G' and G'' behave as a power law in the frequency regime less than Γ_0. The interesting regime is the range where x/x_g lies between 1 and 2. In this range, G' and G'' have a constant ratio and both vary as $\omega^{(x/x_g)-1}$.

3. For frequencies greater than order 1 relative to the attempt frequency, we do not see the extension of the power law behavior, but instead, we see an equivalent of a relaxation peak at a frequency of Γ_0 – a point completely in-line with the underlying assumptions of the model which are based upon a mesoscopic mechanism at this frequency. The variation of G' with ω becomes flat or unchanged at approximately Γ_0. The variation of G'' with ω shows that it attains a peak at approximately Γ_0 and has negative curvature in the log-log representation.

5 Comparison of Cytoskeleton and Soft Glassy Materials

It has been hypothesized that cytoskeleton can be considered a SGM [6] and modeled using the SGR theory. Here we examine this hypothesis in the light of the theory review presented above. The main features that are common to the cytoskeleton and the soft glassy materials are:

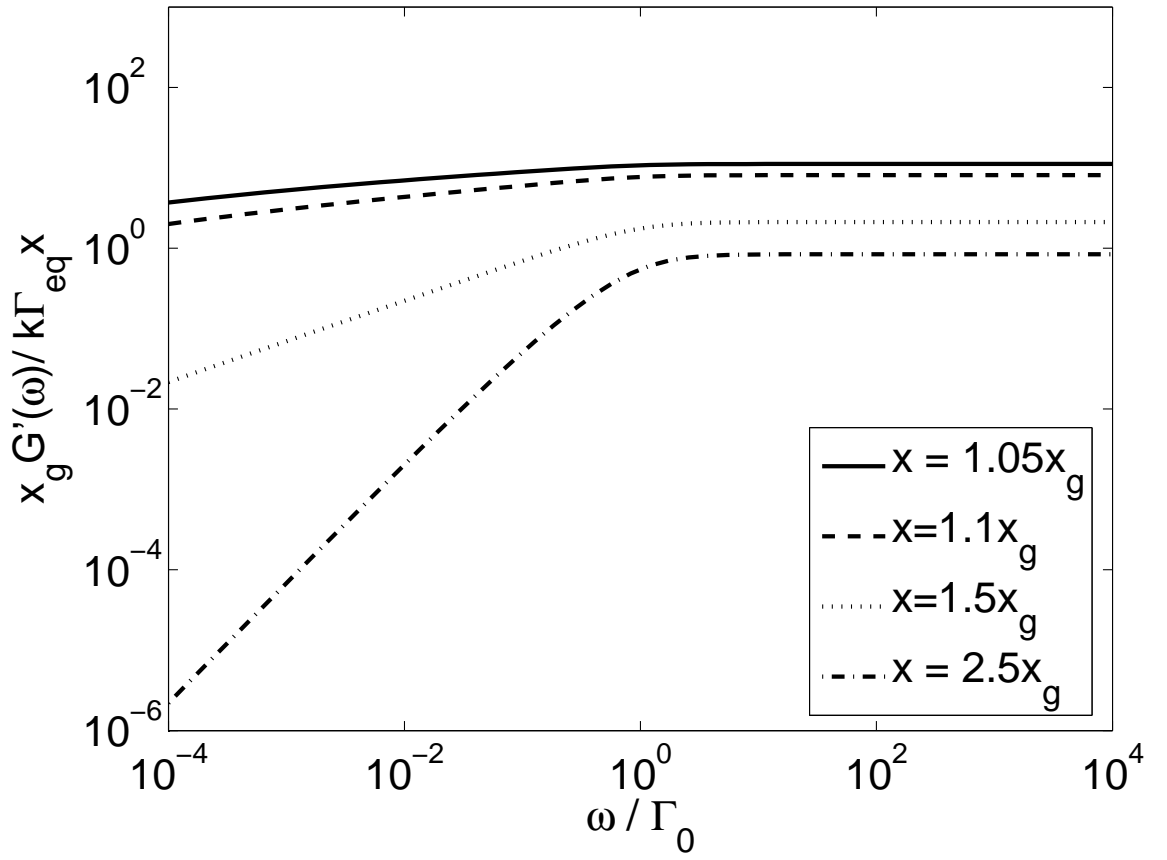1. They are soft (with stiffness in the range of Pa to kPa).

Figure 5: $G^{'}$ variation with frequency ω for $\frac{x}{x_g} = 1.05,\ 1.1,\ 1.5,\ 2.5$.
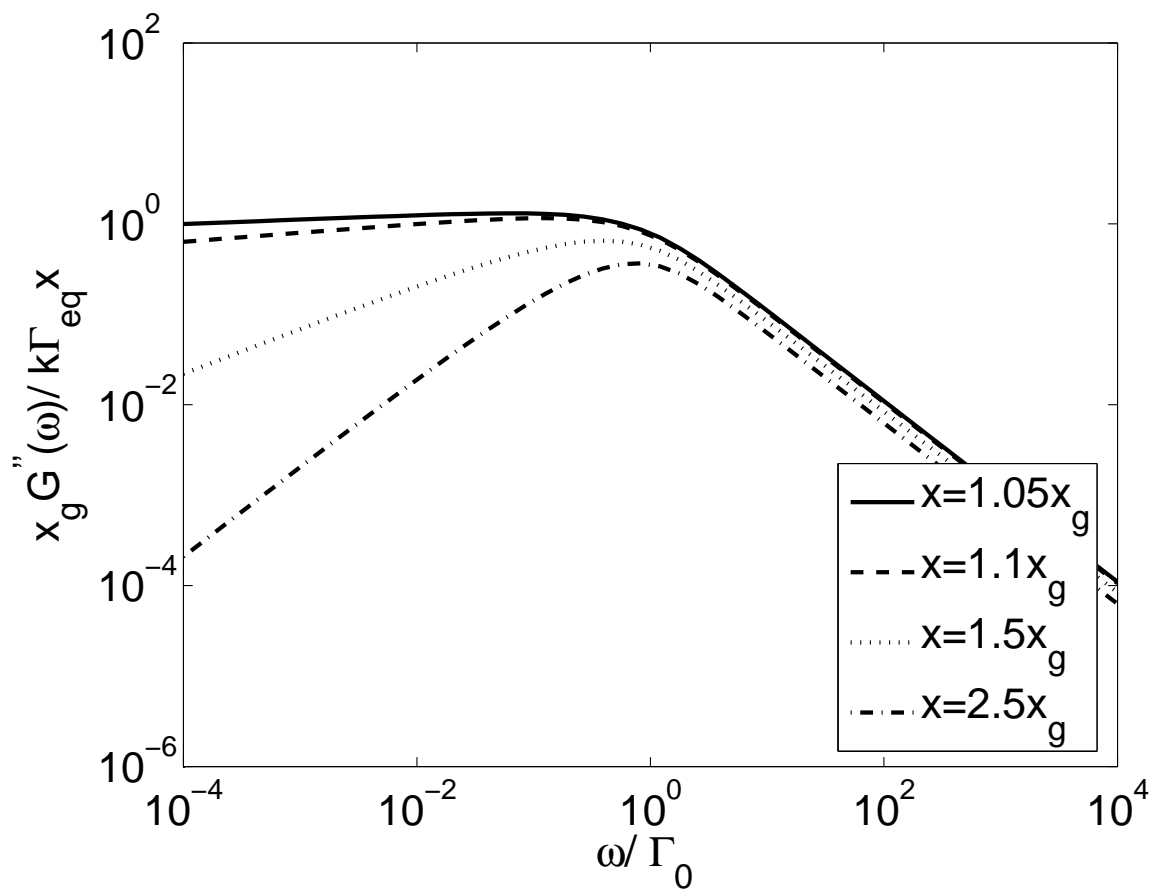
Figure 6: G'' variation with frequency ω for $\frac{x}{x_g} = 1.05$, 1.1, 1.5, 2.5.

20

2. Both the storage modulus and the loss modulus increase with weak power-law dependences on frequency.

3. The loss tangent is generally frequency insensitive.

5.1 Viscoelastic Function Comparison

While there are certain similarities between the rheological response of cytoskeleton and the SGR model, when compared across a wider range of model behaviors this similarity disappears altogether.

5.1.1 Storage Modulus

The storage modulus G' from the data and the SGR model match each other well over the known data range. However, it is noted that the data do not extend to near $\omega/\Gamma_0 \sim 1$, where the SGR model predicts an upper bound to the storage modulus; see Figs. 3 and 5 and note that $\Gamma_0 \sim 10^8$ 1/sec. This promising behavior also gives us the interpretation that mechanistically the cytoskeleton possesses a linear log-log relaxation-time spectra. But caution is advised since the range of the collected data is limited relative to the interesting features of the SGR model.

5.1.2 Loss modulus

A comparison of the G'' behavior of the model and the data, however, show a clear problem. The SGR model predicts a decrease of G'' with frequency for $\omega/\Gamma_0 > 1$ (see Fig. 6) and over its entire range (on a log-log scale) it is concave. The data follow an opposite trend even well below $\omega/\Gamma_0 \sim 1$; see Fig. 3. One could argue that this defect of the SGR model is repairable by the addition of a term proportional to $\delta(t)$ to Eq. (34). However, this would then break the connection to the SGR model which was precisely formulated to possess many important theoretical features.

5.1.3 Loss Tangent

The loss tangent from the SGR model is monotonically decreasing and decreases rapidly for frequencies ω/Γ_0 of order unity. Cytoskeleton data, however, display an opposite trend (primarily due to the above mentioned discrepancy with the loss modulus). This situation is repairable in the same fashion as mentioned above but then one loses the connection to the SGR model.

5.2 Non-equilibrium Issues: Aging

One of the most striking features that might make the cytoskeleton characterization similar to soft glassy materials is aging. For $x < x_g$ the SGR

model displays aging behaviors, and, in recent experimental results [3], indicators of aging in cytoskeletal mechanical response have been measured. [3] provides experiments that attempt to characterize aging, rejuvenation and remodeling events in cytoskeleton. One of the basic experiments performed shows that a tracer bead attached to the cytoskeleton diffuses in a manner that is inconsistent with equilibrium diffusive behavior (Stokes-Einstein behavior); see Figs. 3 and 4 in [3]. The implication of the observed time scaling behavior is that the cell culture is below its glass transition temperature. However, this brings us to a fundamental inconsistency if we are to accept that the cytoskeleton is a SGM and can be modeled using the SGR theory. Let us assume that the data from [7] represents a control data set and that the cytoskeleton system used in the bead tracer experiments in [3] is in a similar state of preparation. We observe that a good data fit was obtained in [7] with $x/x_g = 1.2$. According to the SGR model, this means that the system is above its glass transition temperature. In such a state, however, we would not in general expect to see evidence of aging of the type observed in [3]. One could hypothesize that the cell culture in [3] was above its glass transition temperature but was prepared well out of its equilibrium state. It is, however, noted that it is shown (via creep experiments – see Fig. 1 in [3]) that the system displays out of equilibrium behavior for over 8000 seconds. The value of Γ_0 which fits the data of [7] well is of the order of 10^8 1/sec. This would indicate that the system was prepared exceedingly far from equilibrium; it would in fact need to be in a state which would have an equilibrium probability of order 10^{-11}. Thus the likelihood of this scenario is quite low and we are left with a fundamental inconsistency between the data and the SGR model.

6 Concluding Remarks

The modeling of the rheological behavior of the cytoskeleton is very challenging subject and in this paper we have attempted to shed some light on the standard structure of rheological models, the SGR model in particular, and their relation to the experimental response of cytoskeleton. We have clearly raised more questions than we have answered, but we are confident in stating that the SGR model, in its *present formulation*, is not adequate for describing the behavior of cytoskeleton. We base our conclusion on the following two points:

1. The loss behavior of the SGR model deviates from the measured loss behavior in cytoskeleton. The curvature of the loss measures (loss modulus or loss tangent) have opposite sign as that of the data. This fundamental discrepancy points to the action of distinctly differing local physics.

2. If one is willing to overlook point one, then one is forced to accept that as a SGR system, cytoskeleton is in a state above above its (abstract) glass transition temperature. One the other hand, the collected data also indicates non-equilibrium behavior of the aging type which indicates that the system is in a glassy state. The discrepancy is difficult to resolve even if one is willing to accept the existence of a non-equilibrium preparation above the glass transition.

The SGR model is a beautiful and complete theory of viscoelastic behavior but it possess a very particular assumed structure of the underlying physics of the system. It appears, unfortunately, that cytoskeleton is not fully compatible with these assumptions. From the viewpoint of modeling, it is important that any model, one attempts to apply to a system, provide insight into its behavior and provide predictive capabilities. Else, one is simply performing an exercise of curve fitting. The SGR model was very attractive in this sense but on close inspection it does not hold up relative to the cytoskeleton data. We are, thus, still in search of a model. Important features for such a model which we identify from our study include:

1. Over certain ranges of frequency we should have power law storage and loss moduli but that above some frequency we should start to see increasing dissipation. In this regard it would be very useful to collect higher frequency data to ascertain further trends in the data.

2. The model should be able to distinguish between above and below glass transition states. In particular, it should ideally possess a sub-scale dynamic component to allow one to model non-equilibrium behaviors. This could be in the form of an evolution equation as in the SGR framework or it could involve the use of relaxation kernels that do not possess the assumption of TTI and thus have an explicit argument that accounts for the state of the system in terms of the total time since preparation. Additional characterizations which attempt to ascertain the dependencies of system response in terms of time since preparation will be very helpful in furthering this effort.

7 Acknowledgments

References

[1] A.S. Argon, *Theory for low-temperature plastic-deformation of glassy polymers*, Philosophical Magazine **28** (1973), 839–865.

[2] J.P. Bouchaud, *Weak ergodicity breaking and aging in disordered systems*, Journal de Physique I France **2** (1992), 1705–1713.

[3] P. Bursac, G. Lenormand, B. Fabry, M. Oliver, D.A. Weitz, V. Viasnoff, J.P. Bulter, and J.J. Fredberg, *Cytoskeletal remodeling and slow dynamics in the living cell*, Nature Materials **4** (2005), 557–561.

[4] M. Cloitre, R. Borrega, and L. Leibler, *Rheological aging and rejuvenation in microgel pastes*, Physical Review Letters **85** (2000), 4819–4822.

[5] L. Deng, X. Trepat, J.P. Butlet, E. Millet, K.G. Morgan, D.A. Weitz, and J.J. Fredberg, *Fast and slow dynamics of the cytoskeleton*, Nature Materials **5** (2006), 636–640.

[6] B. Fabry, G.N. Maksym, J.P. Bulter, M. Glogauer, D. Navajas, and J.J. Fredberg, *Scaling the microrheology of living cells*, Physical Review Letters **87** (2001), 14102.

[7] B. Fabry, G.N. Maksym, J.P. Bulter, M. Glogauer, D. Navajas, N.A. Taback, E.J. Millet, and J.J. Fredberg, *Time scale and other invariants of integrative mechanical behavior in living cells*, Physical Review E **68** (2003), 041914.

[8] J.D. Ferry, *Viscoelastic properties of polymers*, John Wiley and Sons, 1961.

[9] R.M. Fuoss and J.G. Kirkwood, *Electical properties of solids. VIII. Dipole moments in polyvinyl chloride-diphenyl systems*, Journal of the American Chemical Society **63** (1941), 385–394.

[10] A.E. Green and R.S. Rivlin, *The mechanics of non-linear materials with memory. Part I.*, Archive for Rational Mechanics and Analysis **1** (1957), 1–21.

[11] H. Hoffman and A. Rauscher, *Aggregating systems with a yield stress value*, Colloid Polymer Science **271** (1993), 390–395.

[12] S.A. Khan, R.K. Prudhomme, and W.W. Graessley, *Rheology of concentrated microgel solutions*, Rheologica Acta **27** (1988), 531–539.

[13] S.A. Khan, C.A. Schnepper, and R.C. Armstrong, *Foam rheology: III. Measurement of shear flow properties*, Journal of Rheology **32** (1988), 69–92.

[14] C. T. Lim, E. H. Zhou, and S. T. Quek, *Mechanical models for living cells*, Journal of Biomechanics **39** (2006), 195–216.

[15] M. R. Mackley, R.T.G. Marshall, J.B.A.F. Smeulders, and F.D. Zhao, *The rheological characterization of polymeric and colloidal fluids*, Chemical Engineering Science **49** (1994), 2551–2565.

[16] T.G. Mason, J. Bibette, and D.A. Weitz, *Elasticity of compressed emulsions*, Physical Review Letters **75** (1995), 2051–2054.

[17] T.G. Mason and D.A. Weitz, *Linear viscoelasticity of the colloidal hard sphere suspensions near the glass transition*, Physical Review Letters **75** (1995), 2770–2773.

[18] M.R.K. Mofrad and R.D. Kamm, *Cytoskeletal mechanics: Models and measurements*, Cambridge University Press, 2006.

[19] C. Monthus and J.P. Bouchaud, *Models of traps and glass phenomenology*, Journal of Physics A **29** (1996), 3847–3869.

[20] P. Panizza, D. Roux, V. Vuillaume, C.Y.D. Lu, and M.E Cates, *Viscoelasticity of onion phase*, Langmuir **12** (1996), 248–252.

[21] Physiome Project, `http://www.physiome.org`.

[22] L. Ramos and L. Cipelletti, *Ultraslow dynamics and stress relaxation in the aging of a soft glassy system*, Physical Review Letters **87** (2001), 245503.

[23] P. Sollich, *Rheological constitutive equation for a model of soft glassy materials*, Physical Review E **58** (1998), 738–759.

[24] P. Sollich, F. Lequeux, P. Hebraud, and M.E. Cates, *Rheology of soft glassy materials*, Physical Review Letters **78** (1997), 2020–2023.

[25] L.C.E Struik, *Volume relaxation in polymers*, Rheologica Acta **5** (1966), 303–310.

[26] N.W. Tscheogel, *The phenomenological theory of linear viscoelastic behavior an introduction*, Springer-Verlag, 1989.

[27] E.A. Weeks and D.A. Weitz, *Subdiffusion and the caging effect near the colloidal glass transition*, Chemical Physics **284** (2002), 361–367.